STATE OF THE CLIMATE IN 2019

THE TROPICS

H. J. Diamond and C. J. Schreck, Eds.

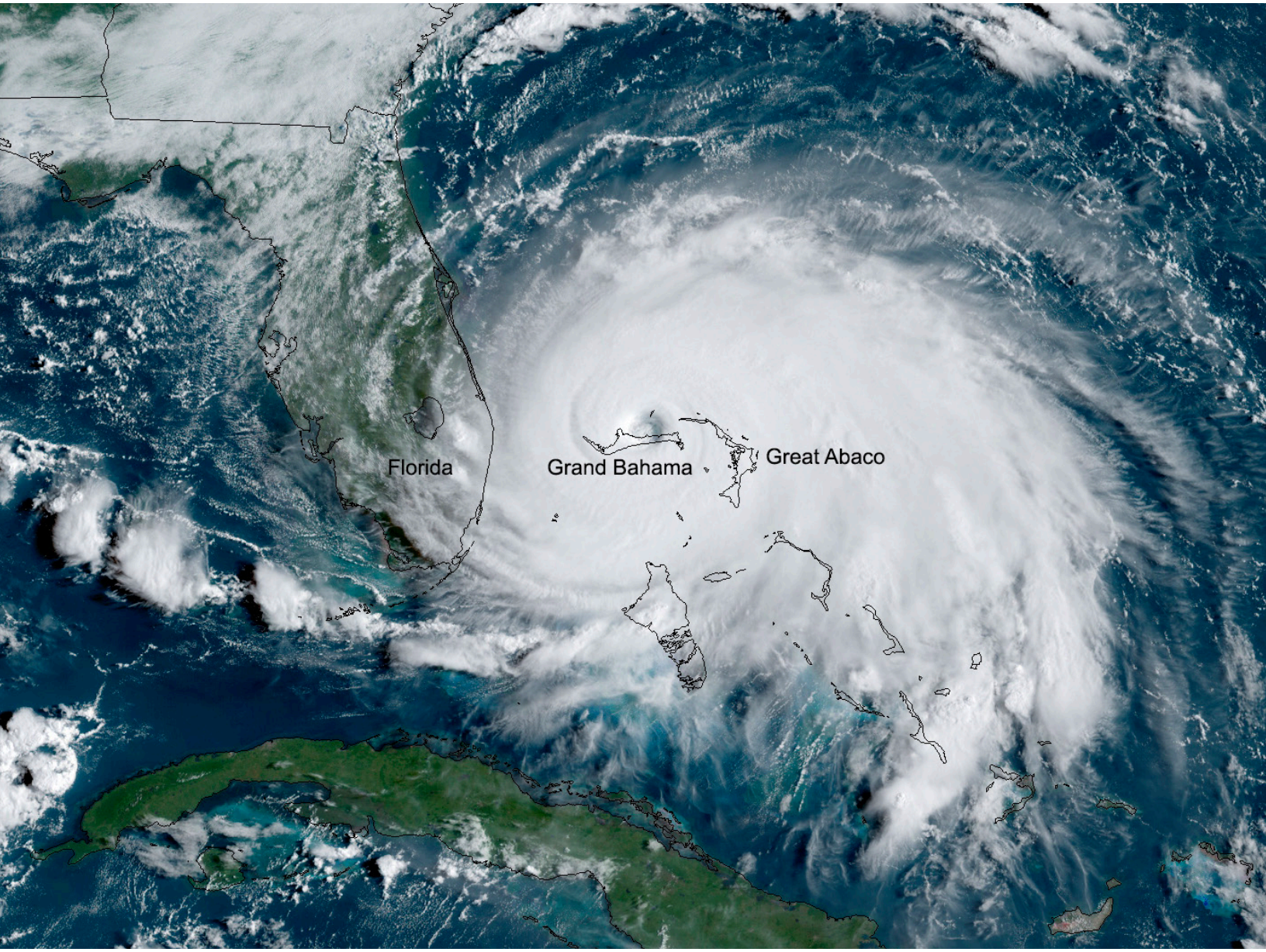

Special Online Supplement to the *Bulletin of the American Meteorological Society,* Vol.101, No. 8, August, 2020

https://doi.org/10.1175/BAMS-D-20-0077.1

Corresponding author: Howard J. Diamond / howard.diamond@noaa.gov

In sections 4f2–4f8, 2018/19 and 2019 seasonal TC activity is described and compared to the historical record for each of the seven WMO-defined hurricane basins. For simplicity, all counts are broken down by the U.S. Saffir–Simpson Hurricane Wind Scale (SSHWS). The overall picture of global TCs during 2019 is shown in Fig. 4.17; actual counts by category are documented in Table 4.2.

Table 4.2. Global counts of TC activity by basin for 2019. "+" means top tercile; "++" is top 10%; "–" is bottom tercile; "––" is bottom 10% (all relative to 1981–2010). "+++" denotes record values for the entire IBTrACS period of record. Please note that some inconsistencies between Table 4.2 and the text of the various basin write-ups in section f exist and are unavoidable, as tallying global TC numbers is challenging and involves more than simply adding up basin totals, because some storms cross TC basin boundaries, some TC basins overlap, and multiple agencies are involved in tracking and categorizing TCs.

Basin	TCs	HTCs	Major HTCs	SS Cat 5	ACE ($\times 10^4$ kt^2)
North Atlantic	18 +	6	3 +	2 ++	130
Eastern North Pacific	19	7	4	0	97
Western North Pacific	27	16	10	3 +	263
North Indian	8 ++	6 +++	3 +++	0	85 +++
South Indian	11 +	10 ++	8 +++	0	154 ++
Australian Region	7 –	4	3 +	0	68
Southwest Pacific	6	4 +	0 –	0	25
Global Totals	**96** ++	**53** +	**31** ++	**5** +	**795**

Globally, five storms during the year reached SSHWS Category 5 strength (sustained wind speeds ≥ 137 kt or 70.5 m s^{-1}). This was one fewer than recorded in 2016 (Diamond and Schreck 2017), equal to the number recorded in 2017 (Diamond and Schreck 2018), and six fewer than the total of 11 recorded in 2018 (Diamond and Schreck 2019). The all-time record of 12 Category 5 global TCs was set in 1997 (Schreck et al. 2014).[1]

The five Category 5 storms were: Super Typhoons Wutip, Hagibis, and Halong in the western North Pacific and Hurricanes Dorian and Lorenzo in the North Atlantic. Dorian caused unprecedented and tremendous devastation, with approximately 70 fatalities reported in the northwest Bahamas and over $3.4 billion (U.S. dollars) in damages generated there. Dorian was responsible for six fatalities in Florida and three in North Carolina and caused over $1 billion (U.S. dollars) in damages in the United States. As a post-tropical cyclone, Dorian also caused considerable damages in Nova Scotia, Canada, with over $100 million (U.S. dollars) in damages reported. While Lorenzo was a Category 5 storm for a short period of time, it was more deadly as a post-tropical/extratropical cyclone. Lorenzo produced tropical storm force winds across portions of Ireland, and was the second deadliest storm of the 2019 North Atlantic season, causing 19 deaths both at sea and along the U.S. coast as a result of high-surf conditions. Sidebar 4.1 details the record-setting and devastating local impacts of Hurricane Dorian.

2) Atlantic basin—G. D. Bell, E. S. Blake, C. W. Landsea, M. Rosencrans, H. Wang, S. B. Goldenberg, and R. J. Pasch

(I) 2019 SEASONAL ACTIVITY

The 2019 Atlantic hurricane season produced 18 named storms, of which six became hurricanes and three achieved major hurricane status (Fig. 4.18a). The HURDAT2 1981–2010 seasonal averages (included in IBTrACS) are 11.8 named storms, 6.4 hurricanes, and 2.7 major hurricanes (Landsea and Franklin 2013). The 2019 seasonal Accumulated Cyclone Energy (ACE) value (Bell et al. 2000) was 134% of the 1981–2010 median (which is 92.4 × 10^4 kt^2; Fig. 4.18b), above NOAA's threshold

[1] SSHWS is based on 1-minute averaged winds, and the categories are defined at: https://www.weather.gov/mfl/saffirsimpson; the Australian category scale is based on 10-minute averaged winds, and those categories are defined at: https://australiasevereweather.com/cyclones/tropical_cyclone_intensity_scale.htm

(120%) for an above-normal season. The numbers of named storms and major hurricanes were also both above average. Therefore, the 2019 season was designated as above normal by NOAA. This makes 2019 the fourth consecutive above-normal season, tying the record set in 1998–2001. This also marks the 17th above-normal season of the 25 since the current Atlantic high-activity era began in 1995 (Goldenberg et al. 2001; Bell et al. 2019).

The previous high-activity era for which fairly reliable data on TC counts and overall hurricane strengths exist is 1950–70. That period also featured numerous above-normal seasons (10 out of 21), while the intervening low-activity era of 1971–94 had only 2 out of 24 (Bell et al. 2018). Note that the hurricane record is considered far less reliable before 1950, with exact season-to-season comparisons for ACE considered less reliable before the mid-1970s and the start of the geostationary satellite era (Landsea et al. 2006). Given these caveats, the best estimates suggest that the previous high-activity era actually spanned the period from 1926–70 (Goldenberg et al. 2001).

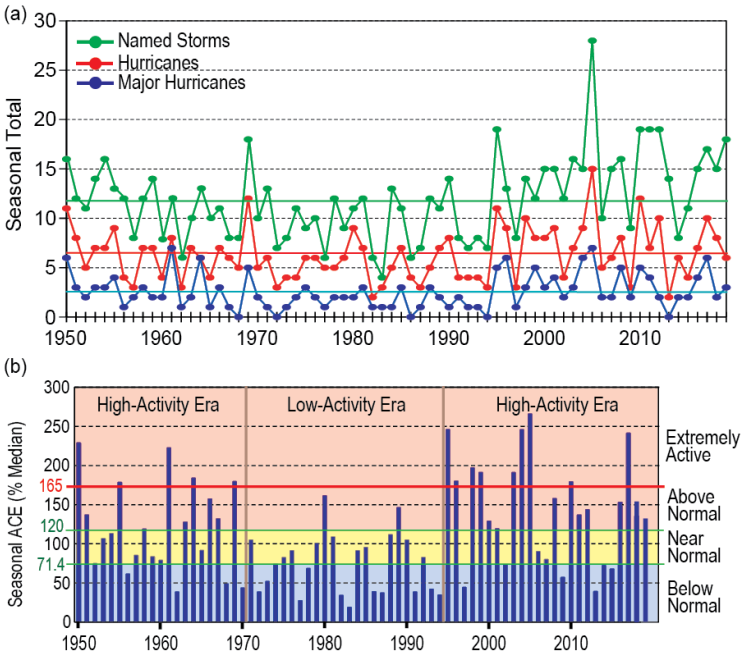

Fig. 4.18. Seasonal Atlantic hurricane activity during 1950–2019. (a) Numbers of named storms (green), hurricanes (red), and major hurricanes (blue); 1981–2010 seasonal means shown by solid colored lines. (b) ACE (Bell et al. 2000) index expressed as percent of the 1981–2010 median value. Red, yellow, and blue shadings correspond to NOAA classifications for above-, near-, and below-normal seasons, respectively (http://www.cpc.ncep.noaa.gov/products/outlooks/background_information.shtml). Thick red horizontal line at 165% ACE value denotes the threshold for an extremely active season. Vertical brown lines separate high- and low-activity eras. Note: There is a low bias in activity during the 1950s to the early 1970s due to the lack of satellite imagery and technique (Dvorak) to interpret TC intensity for systems over the open ocean. (Source: HURDAT2 [Landsea and Franklin 2013] for TC counts.)

The 18 named storms during 2019 are the sixth highest on record since 1950, while the 2019 ACE value is only the 24th highest in that 69-year record. This disparity is in part because two storms (Category 5 Hurricanes Dorian and Lorenzo) produced about 60% of the season's ACE. Meanwhile, eight of the named storms were very short-lived (<2 days). There has been a large artificial increase in these "shorties" since 2000, with seasons averaging about five per year since that time (Landsea et al. 2010). The increased ability to record these storms primarily reflects new observational capabilities such as scatterometers, Advanced Microwave Sounding Units, and the Advanced Dvorak Technique. Villarini et al. (2011) confirmed the lack of association of the shorties' time series with any known climate variability.

(II) STORM FORMATION REGIONS AND LANDFALLS

The vast majority of Atlantic TCs typically form during the peak months (August–October, ASO) of the hurricane season. During 2019, 15 of the 18 named storms, five of the six hurricanes, and all three major hurricanes formed during ASO.

Historically, the primary cause for an above-normal season is a sharp increase in activity associated with storms that form within the Main Development Region (MDR), which spans the tropical Atlantic Ocean and Caribbean Sea between 9.5°N and 21.5°N (Goldenberg and Shapiro 1996; Goldenberg et al. 2001; Bell and Chelliah 2006; Bell et al. 2017, 2018, 2019). For above-normal seasons during 1981–2010, the ACE value associated with storms first named in the MDR averaged 155% of the median (Fig. 4.19a), compared to only 15.8% during below-normal seasons. During 2019, the MDR-related ACE value was 101% of the median.

The nearly tenfold increase in ACE that occurs on average during above-normal seasons reflects the fact that far more MDR-initiated storms eventually become hurricanes (6.4 compared to 1.0) and major hurricanes (4.4 compared to 0.4). These differences not only reflect a nearly four-fold increase in the number of named storms that form within the MDR during above-normal seasons (9.3 compared to 2.5), but also a significantly higher percentage of those storms that become hurricanes (72% compared to 39%) and major hurricanes (44% compared to 17%; Fig. 4.19b). These results are consistent with those of Goldenberg et al. (2001), who noted a five-fold increase in the number of Caribbean hurricanes for high- versus low-activity eras. During 2019, six named storms formed within the MDR, with three (50%) eventually becoming hurricanes and two (33%) eventually becoming major hurricanes. Thus, the MDR-related activity during 2019 was relatively modest for an above-normal season in the entire basin, and no Caribbean hurricanes were recorded.

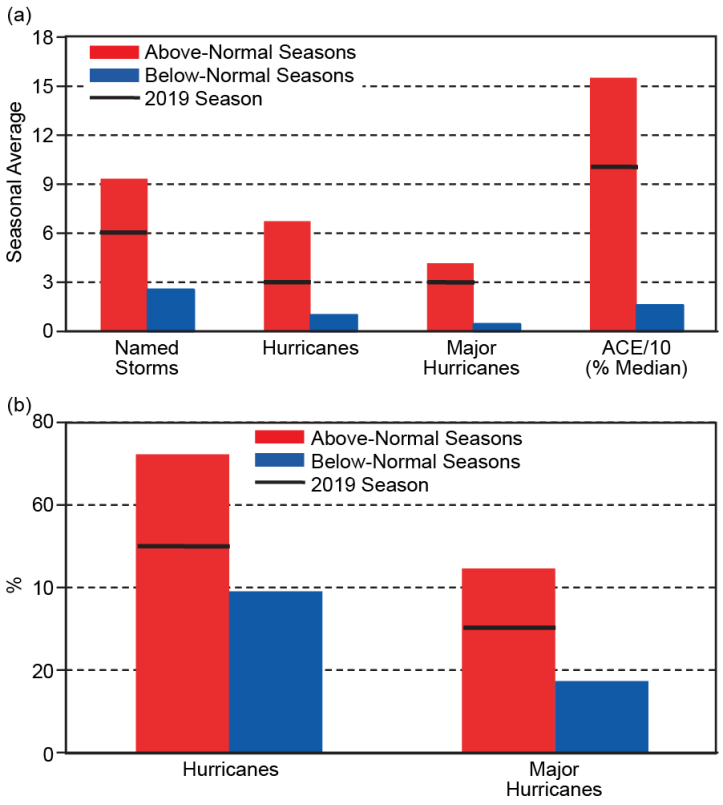

Fig. 4.19. (a) Seasonal averages of specified storm metrics during 1981–2010 associated with named storms initiated within the MDR. (b) Percentage of MDR-initiated named storms during 1981–2010 that eventually became hurricanes (left) and major hurricanes (right). Red (blue) bars show results for above-normal (below-normal) seasons. (Source: HURDAT2 [Landsea and Franklin 2013].)

Two-thirds (67%) of the named storms during 2019 formed outside of the MDR, which is a far higher percentage than the 1981–2010 average of 42% for above-normal seasons. Five of those storms during 2019 formed over the Gulf of Mexico, tying a record with 2003 and 1957 for the most storms to form in that region. The other seven named storms (including one hurricane) during 2019 formed over the North Atlantic north of the MDR, with all but one tropical storm forming over the western North Atlantic (west of 55°W and north of 21.5°N). A relatively high level of TC formation (six named storms including two hurricanes) also occurred over the western North Atlantic in 2018 (Bell et al. 2019).

Regarding landfalls, the most significant landfalling storm of the 2019 Atlantic hurricane season was Major Hurricane Dorian, which stalled over Abaco Island and Grand Bahama Island in the northwest Bahamas during 1–2 September. Dorian spent much of this period at Category 5 intensity, resulting in widespread destruction and death. Dorian tied the Labor Day 1935 hurricane for the strongest on record to make landfall (based on maximum wind speed) anywhere in the Atlantic basin. While the intensity of Dorian was continually observed via satellite and extensively measured by numerous NOAA and Air Force Reserve aircraft reconnaissance flights, the intensity of the 1935 Labor Day storm was only approximated based on a reading from a single land-based barometer, and the estimated maximum surface wind speed was derived using pressure-wind relationships from that one observation.

By 6 September, Dorian weakened to a Category 1 hurricane and made landfall in North Carolina. Two other storms also made landfall in the United States during 2019. These storms were Barry, which made landfall as a Category 1 hurricane in Louisiana on 13 July, and Tropical Storm Imelda, which made landfall in Texas on 17 September.

(III) SEA SURFACE TEMPERATURES

The MDR sea surface temperatures (SSTs) were above average with an area-averaged SST anomaly of +0.40°C (Fig. 4.20b). Most locations had departures between +0.25°C and +0.50°C. However, this anomaly was only slightly higher (by 0.1°C) than the remainder of the global tropics (Fig. 4.20c).

On multi-decadal time scales, the presence of higher SST anomalies in the MDR compared to the global tropics typifies the warm phase of the Atlantic Multidecadal Oscillation (AMO; Enfield and Mestas-Nuñez 1999; Bell and Chelliah 2006) and is characteristic of Atlantic high-activity eras such as 1950–70 and 1995–present (Goldenberg et al. 2001; Vecchi and Soden 2007; Bell et al. 2018). On interannual time scales, large fluctuations in the relative anomalous warmth of the MDR can also be seen. This variability can have nothing to do with the AMO itself and instead reflect factors such as fluctuations in the wind patterns across the MDR, El Niño–Southern Oscillation (ENSO), the Pacific-Decadal Oscillation, and Indian Ocean SST variability. During ASO 2019, area-averaged SSTs in both the tropical Indian and tropical Pacific Oceans were the second highest (anomalies were +0.73°C and +0.50°C, respectively) in the 1950–2019 record. The reduction in the relative anomalous MDR warmth, especially when compared to most years since 1995, reflected these conditions and should not be interpreted as an indicator that the warm AMO phase has ended.

Another important SST signal during ASO reflected above-average SSTs in the western North Atlantic (red box, Fig. 4.20a), where six TCs formed. The area-averaged SST anomaly in this region (+0.60°C) indicates a continuation of exceptional warmth in that area that began in 2014 (Fig. 4.20d).

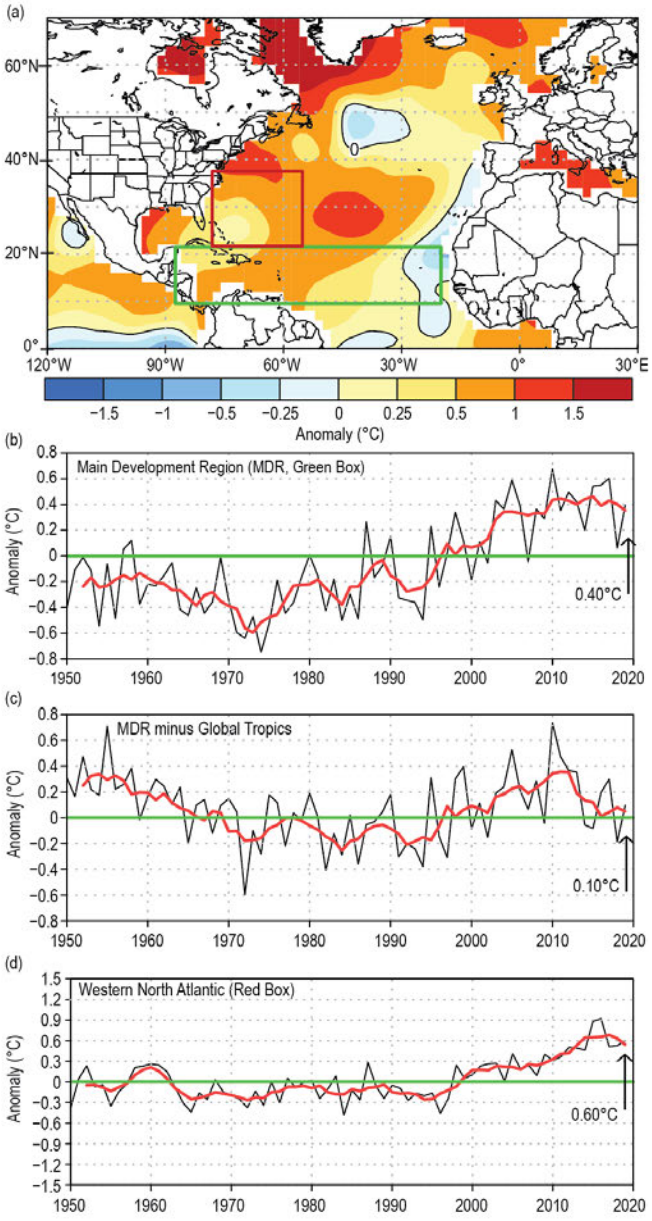

Fig. 4.20. (a) Aug–Oct (ASO) 2019 SST anomalies (°C). (b)–(d) Time series of ASO area-averaged SST anomalies (black) and 5-point running mean of the time series (red): (b) in the MDR (green box in (a), spanning 20°–87.5°W and 9.5°–21.5°N), (c) difference between the MDR and the global Tropics (20°N–20°S), and (d) in the western North Atlantic (red box in (a), spanning 55°–77.5°W and 21.5°–37.5°N). Anomalies are departures from the 1981–2010 period means. (Source: ERSST-v5 [Huang et al. 2017].)

(IV) ATMOSPHERIC CONDITIONS

Consistent with the ongoing high-activity era for Atlantic hurricanes, an interrelated set of conditions during ASO 2019 favored increased TC activity in the MDR even if that region was relatively quiet in 2019. These included upper tropospheric anticyclonic streamfunction anomalies across the subtropical North Atlantic, in association with an enhanced subtropical ridge (Fig. 4.21a). A similar anomaly pattern was present across the subtropical South Atlantic Ocean. This pronounced inter-hemispheric symmetry of the anticyclonic anomalies is typical of an enhanced West African monsoon system (Bell and Chelliah 2006), which is the June–September portion of the North African monsoon.

During 2019, these conditions were associated with upper-level easterly wind anomalies across the MDR and lower-level westerly wind anomalies over the eastern half of the MDR (Fig. 4.21b). This

overall pattern resulted in anomalously weak vertical wind shear across the MDR (Figs. 4.22a,b). The area-averaged magnitude of the vertical wind shear within the MDR was 7.0 m s^{-1} (Fig. 4.22c), which is below the 8 m s^{-1} threshold considered conducive to hurricane formation on a monthly time scale (Bell et al. 2017).

Over the eastern half of the MDR, the lower-level westerly wind anomalies reflected weaker easterly trade winds (Fig. 4.21b). These anomalies extended upward to at least the 700-hPa level (Fig. 4.21c), the approximate level of the African Easterly Jet (AEJ). This contributed to a deep layer of anomalous cyclonic relative vorticity (i.e., increased horizontal cyclonic shear) along the equatorward flank of the AEJ. These conditions are known to favor increased TC activity within the MDR by helping African easterly waves to be better maintained and by providing an inherent cyclonic rotation to their embedded convective cells (Bell et al. 2004, 2006, 2017, 2018).

All of the above conditions are typical of an enhanced West African monsoon system (Gray 1990; Hastenrath 1990; Landsea et al. 1992; Bell and Chelliah 2006; Bell et al. 2018). The strength of that monsoon is a major factor contributing to observed multidecadal fluctuations in Atlantic hurricane activity because it directly impacts atmospheric conditions and TC formation and intensification within the MDR. During August–September, one indicator of the enhanced monsoon was an extensive area of anomalous 200-hPa divergence across western Africa, with an associated core of negative velocity potential anomalies (Fig. 4.23a). Another indicator was enhanced convection (shown by negative Outgoing Longwave Radiation [OLR] anomalies) in the African Sahel region (red box, Fig. 4.23b). During August–September, OLR values in this region averaged 237 W m^{-2} (Fig. 4.23c). Values below 240 W m^{-2} indicate deep tropical convection. These values are typical of the current high-activity era, whereas OLR values generally above 240 W m^{-2} (indicating a weaker monsoon) were typical of the low-activity period of the 1980s and early 1990s. These multidecadal fluctuations in monsoon strength coincide with opposing phases (warm and cold, respectively) of the AMO.

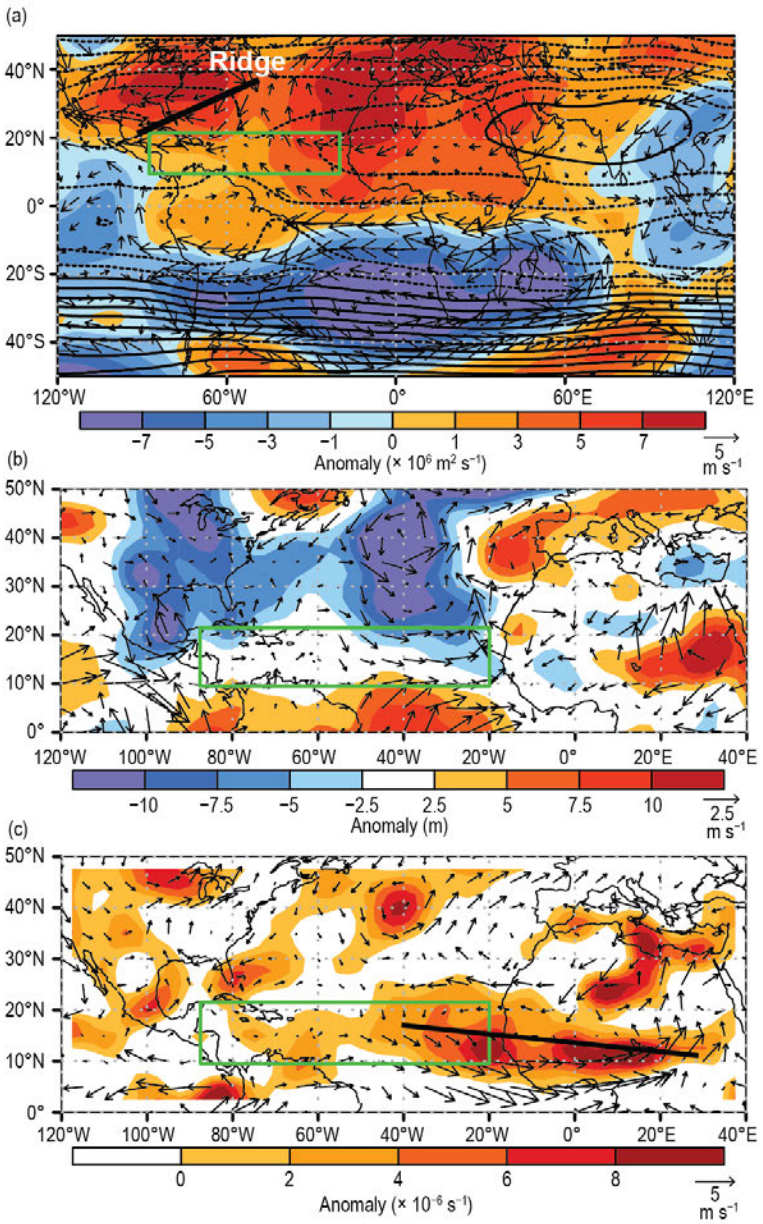

Fig. 4.21. Aug–Oct 2019: (a) 200-hPa streamfunction (contours, interval is 5 × 10^6 m^2 s^{-1}) and anomalies (shaded), and anomalous vector winds (m s^{-1}); (b) anomalous 1000-hPa heights (shaded, m) and vector winds; and (c) anomalous 700-hPa cyclonic relative vorticity (shaded, × 10^{-6} s^{-1}) and vector winds. In (a), the upper-level ridge discussed in the text is labeled and denoted by the thick black line. In (c), the thick solid line indicates the axis of the mean African Easterly Jet, hand-drawn based on total seasonal wind speeds (not shown). Vector scales differ for each panel, and are below right of the color bar. The green box denotes the MDR. Anomalies are departures from the 1981–2010 means. (Source: NCEP–NCAR reanalysis [Kalnay et al. 1996].)

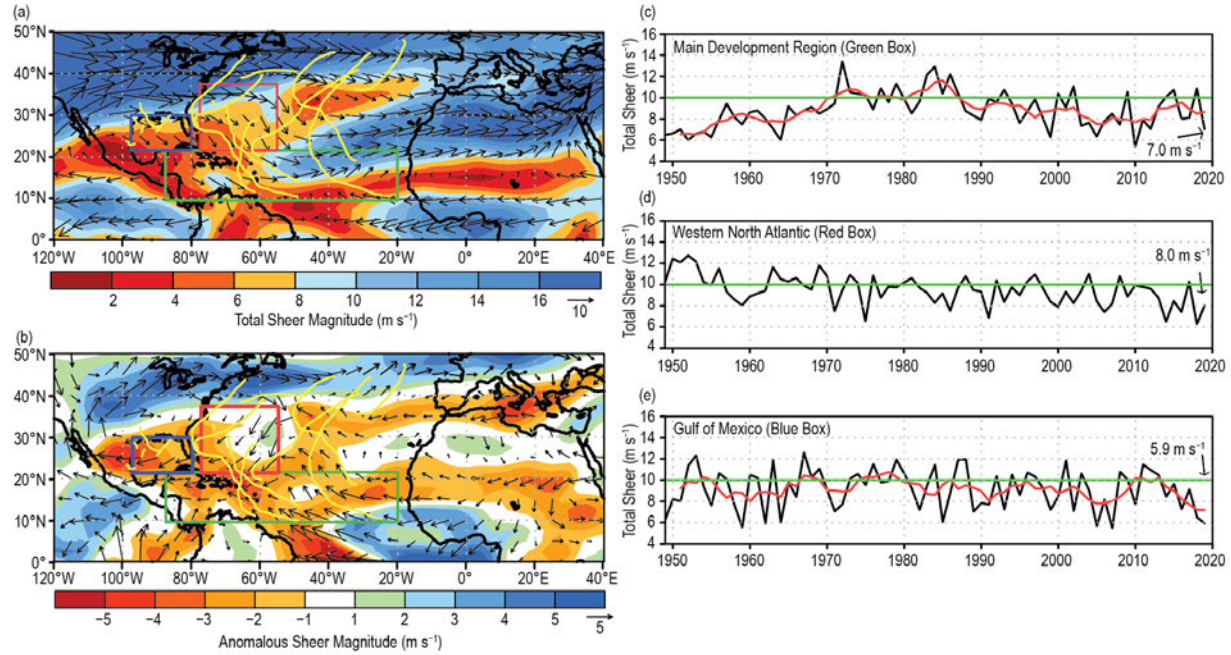

Fig. 4.22. Aug–Oct (ASO) magnitude of the 200–850-hPa vertical wind shear ($m s^{-1}$): (a) 2019 total magnitude and vector and (b) 2019 anomalous magnitude and vector versus 1981–2010 means. (c)–(e) Time series of ASO vertical shear magnitude (black) and 5-point running mean of the time series (red) averaged over (c) the MDR (green box in (a), (b) spanning 87.5°–20°W and 9.5°–21.5°N); (d) the western North Atlantic (red box in (a), (b) spanning 77.5°–55°W and 21.5°–37.5°N); and (e) the Gulf of Mexico (blue box in (a), (b) spanning 97.5°–80°W and 21.5°–30°N). In (a) and (b), 2019 TC tracks (yellow lines) are shown and vector scale ($m s^{-1}$) is below right of color bar. (Source: NCEP–NCAR reanalysis [Kalnay et al. 1996].)

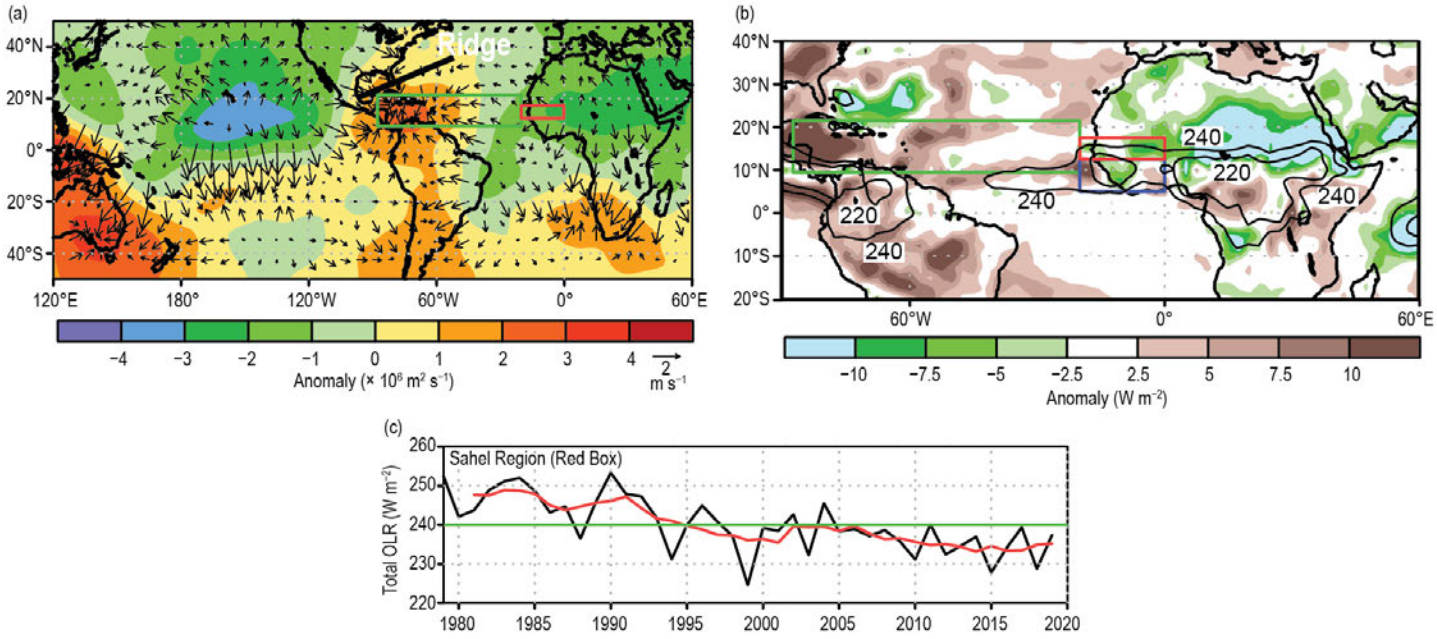

Fig. 4.23. (a) Aug–Sep 2019 anomalous 200-hPa velocity potential (× 10^6 $m^2 s^{-1}$) and divergent wind vectors ($m s^{-1}$). (b) Aug–Sep 2019 anomalous OLR ($W m^{-2}$), with negative (positive) values indicating enhanced (suppressed) convection. (c) Time series of Aug–Sep total OLR (black) and 5-point running mean of the time series (red) averaged over the African Sahel region (red box in (a) and (b) spanning 20°W–0° and 12.5°–17.5°N). In (a) the upper-level ridge discussed in the text is labeled and denoted by the thick black line. In (b), contours show total OLR values of 220 $W m^{-2}$ and 240 $W m^{-2}$. In (a) and (b), the green box denotes the MDR. Anomalies are departures from the 1981–2010 means. (Source: NCEP–NCAR reanalysis [Kalnay et al. 1996] for velocity potential and wind.)

SIDEBAR 4.1: **Hurricane Dorian: A devastating hurricane for the northwest Bahamas—** P. J. KLOTZBACH AND R. E. TRUCHELUT

The 2019 Atlantic hurricane season ended up slightly above normal for most tropical cyclone (TC) parameters, with a total of 18 named storms, six hurricanes, and three major hurricanes occurring. By far, the most significant and devastating hurricane of the 2019 season was Hurricane Dorian. Dorian will be most remembered for the devastation that it caused in the northwest Bahamas, especially on the Abaco Islands and on Grand Bahama Island. It was also the longest-lived (14 days as a named storm and 10 days as a hurricane) and most intense (1-minute maximum sustained winds of 160 kt (82 ms^{-1}) hurricane of the 2019 season (Avila et al. 2020). Dorian also generated the most Accumulated Cyclone Energy (ACE) of any Atlantic hurricane, accounting for ~40% of basinwide ACE accrued in 2019. This sidebar summarizes the meteorological history of Dorian along with the notable records that the hurricane achieved during its track across the Atlantic. Historical landfall records from 1851–present are taken from the National Hurricane Center/Atlantic Oceanographic and Meteorological Laboratory archive located at: http://www.aoml.noaa.gov/hrd/hurdat/All_U.S._Hurricanes.html, and Dorian's observed values are taken from Avila et al (2020).

Dorian became a tropical depression (TD) on 24 August in the central tropical Atlantic and was upgraded to a tropical storm (TS) shortly thereafter (Fig. SB4.1). Despite moving through an environment of relatively low wind shear and a warm sea surface (~28°–29°C), considerable mid-level dry air inhibited Dorian's intensification early in its lifetime. Dorian passed through the Windward Islands on 27 August as a TS. Dorian's center reformed farther north after interacting with Saint Lucia, and its center also reformed downshear (i.e., to the east) due to moderate westerly shear. This northeastward shift in track from where the models were originally forecasting the storm allowed it to avoid the elevated terrain of Hispaniola and Puerto Rico, which would have likely weakened the storm. It then turned northwestward and intensified as it moved into a more moisture-rich environment. Dorian became a hurricane as it tracked over Saint Croix on 28 August and reached major hurricane intensity on 30 August as it approached the Bahamas.

From 0600 UTC on 30 August to 1800 UTC on 31 August, Dorian underwent rapid intensification from 90 kt (46 ms^{-1}) to 130 kt (67 ms^{-1}) with 24-hour intensification rates ranging between 30 kt (15 ms^{-1}) and 35 kt (18 ms^{-1}). Dorian slowed as it approached the northwest Bahamas, then underwent another burst of rapid intensification, becoming a Category 5 hurricane as it approached Great Abaco Island.

Soon thereafter, Dorian reached its maximum intensity of 160 kt (82 ms^{-1}) as it made landfall on Great Abaco Island on 1 September. In doing so, Dorian became the strongest hurricane on record to make landfall in the Bahamas and tied with the Labor Day Hurricane of 1935 for the strongest landfalling hurricane on record anywhere in the Atlantic basin. The 160 kt (82 ms^{-1}) intensity achieved by Dorian was also the strongest on record by any Atlantic hurricane outside of the tropics (>23.5°N) in the satellite era (since 1966). Dorian tracked slowly over Great Abaco as the steering currents collapsed, and the system effectively stalled after making landfall on Grand Bahama Island with maximum sustained winds of 155 kt (80 ms^{-1}) (Fig. SB4.2). Dorian was the first Category 5 hurricane on record to make landfall on Grand Bahama Island. Its extremely slow forward movement caused devastating wind, rain, and storm surge impacts over these islands. During its first 24 hours over Grand Bahama Island, Dorian

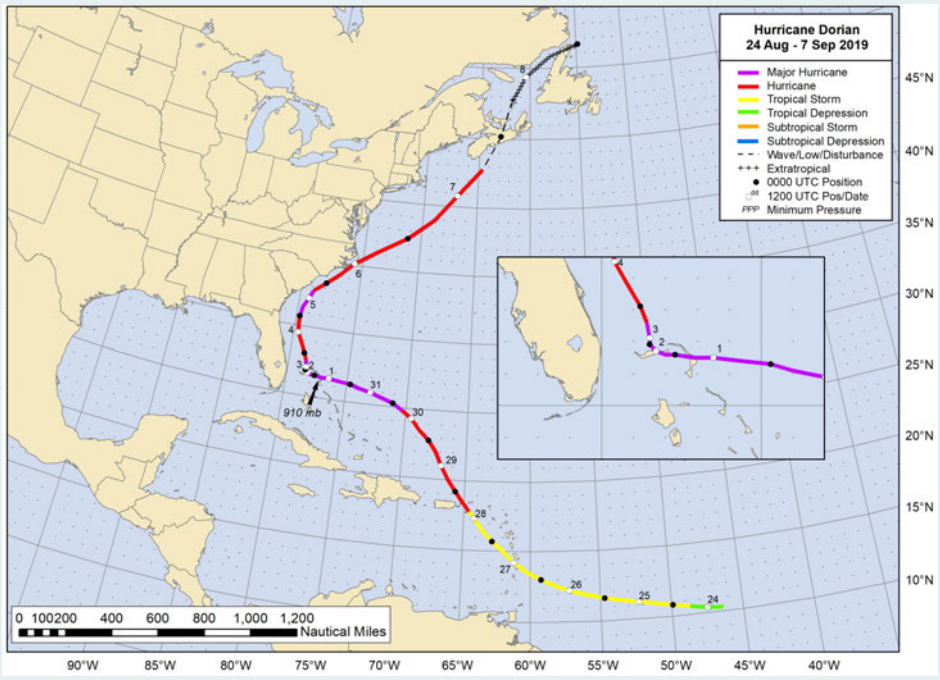

Fig. SB4.1. NOAA's National Hurricane Center Best Track Plot for Hurricane Dorian (Avila et al. 2020).

weakened extremely slowly—from a 155 kt (80 m s^{-1}) Category 5 hurricane to a 115 kt (59 m s^{-1}) Category 4 hurricane. Because of this stalling motion and maintenance of strong hurricane intensity, Dorian generated the most ACE in a 1° × 1° grid box in the Atlantic basin in the satellite era (i.e., since 1966; Wood et al. 2020).

Land interaction, an increase in vertical wind shear, and cold water upwelling continued to slowly reduce Dorian's wind strength, and it weakened below major hurricane strength late on 3 September. Dorian tracked northward offshore of the southeast United States and briefly regained major hurricane strength on 5 September before weakening as it encountered lower sea surface temperatures (SSTs) and stronger vertical wind shear. It brushed the South Carolina and North Carolina coasts, and Dorian made landfall on Cape Hatteras at 1230 UTC on 6 September as a Category 2 hurricane, with winds estimated at 85 kt (44 m s^{-1}), although most of the strongest winds remained over water to the east of the center (Avila et al. 2020). At the time of its North Carolina landfall, Dorian's central pressure was 956 hPa, tying it with Floyd (1999) and Florence (2018) for the sixth lowest central pressure for a landfalling North Carolina hurricane since 1950. Dorian became extratropical as it accelerated northeastward, but it also strengthened slightly during this time. It made a final landfall as a post-tropical cyclone in Nova Scotia on 7 September, bringing hurricane-force winds to portions of Atlantic Canada. Dorian made a final landfall as a post-tropical storm in Newfoundland on 8 September.

Dorian was an extremely long-lived storm and set several records due to both its intensity and longevity. Its 160 kt (82 m s^{-1}) winds were tied with Gilbert (1988) and Wilma (2005) for the second strongest on record for an Atlantic hurricane in the satellite era (since 1966), trailing only the 165 kt (85 m s^{-1}) winds recorded by Allen (1980). Its lifetime minimum central pressure of 910 hPa was tied with Ivan for the ninth-lowest lifetime minimum central pressure since 1980. Dorian generated 49 × 10^4 kt^2 ACE during its lifetime—the fifth most for an August TC in the satellite era. It also generated 14 named storm days, tying it with Felix (1995) for third place for most named storm days by a storm forming in August in the satellite era.

Given its extreme intensity and slow forward speed over both Great Abaco Island and Grand Bahama Island, Dorian caused tremendous devastation, with over 70 fatalities reported by the Bahamian Health Minister and $3.4 billion (U.S. dollars) in damage generated (Avila et al. 2020). Dorian was responsible for four indirect fatalities in the United States and caused $1.6 billion (U.S. dollars) in damage. Dorian as a post-tropical cyclone also caused considerable damage in Nova Scotia, with over $100 million (U.S. dollars) in damage being reported.

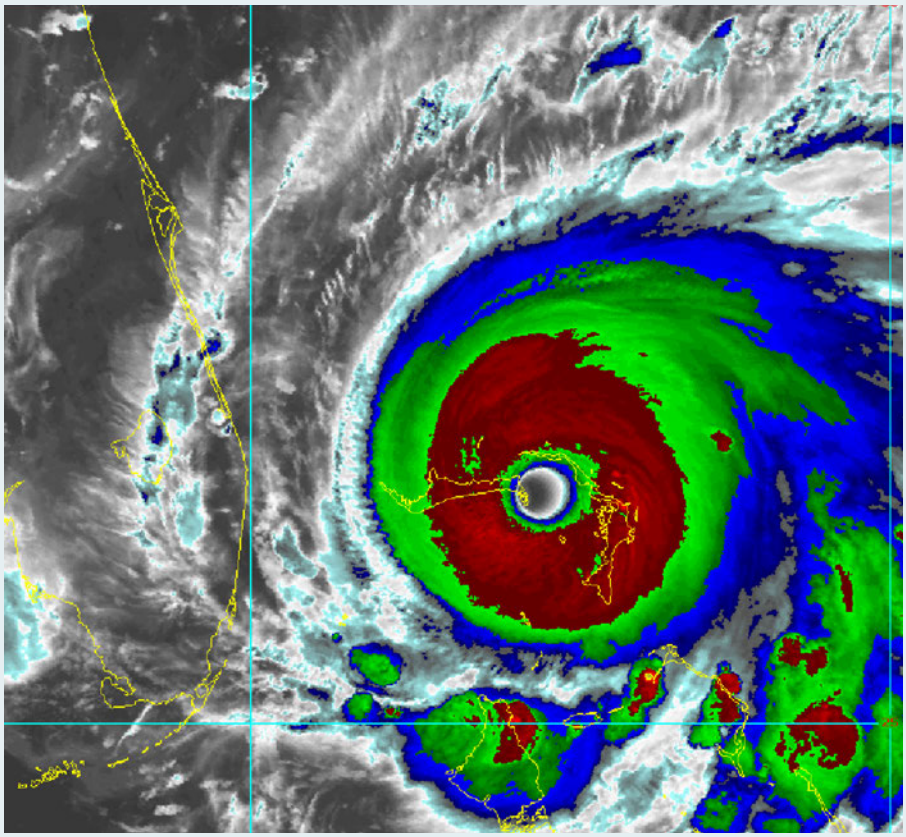

Fig. SB4.2. NOAA-18 infrared satellite image of Hurricane Dorian making landfall on Grand Bahama Island at 154 UTC on 2 Sep 2019.

Despite the above conditions, the 2019 TC activity for the MDR as a whole was relatively modest. This signal partly reflected the limited activity (two tropical storms) over the Caribbean Sea due in part to anomalously strong upper-level convergence (Fig. 4.23a) and sinking motion there. The modest activity was also associated with the synoptic scale sinking motion typically found downstream of the mean ridge axis, which in this case extended across the Gulf of Mexico and western subtropical North Atlantic (indicated by thick black line in Figs. 4.21a, 4.23a).

Two other aspects of the interannual variability during ASO 2019 include the relatively high number of six TC formations over the western subtropical North Atlantic and five over the Gulf of Mexico (yellow lines, Fig. 4.22). These

are roughly double the 1981–2010 averages seen during above-normal seasons. In addition to anomalously warm SSTs during ASO (Fig. 4.20a), both regions experienced below-average vertical wind shear (Fig. 4.22b) with area-averaged shear values at or below 8 m s^{-1} (Figs. 4.22d,e). For the Gulf of Mexico, the area-averaged shear was less than 6 m s^{-1} (Fig. 4.22e), which is comparable to some of the lowest values in the record. These conditions were linked to the persistent, anomalous upper-level ridge that extended across both regions (Fig. 4.21a).

3) Eastern North Pacific and Central North Pacific basins—K. M. Wood and C. J. Schreck

(I) SEASONAL ACTIVITY

Two agencies are responsible for issuing advisories and warnings in the eastern North Pacific (ENP) basin: NOAA's National Hurricane Center in Miami, Florida, covers the region from the Pacific coast of North America to 140°W, and NOAA's Central Pacific Hurricane Center in Honolulu, Hawaii, covers the central North Pacific (CNP) region between 140°W and the date line. This section combines statistics from both regions.

A total of 19 named storms formed in the combined ENP/CNP basin, seven of which became hurricanes and four became major hurricanes. The 1981–2010 IBTrACS seasonal averages for the basin are 16.5 named storms, 8.5 hurricanes, and 4.0 major hurricanes (Schreck et al. 2014). Thus, 2019 storm counts were near normal (Fig. 4.24a). These storms occurred between the official start date of the ENP season of 15 May and end date of 30 November. Hurricane Alvin first reached tropical storm strength on 29 June—the latest first storm formation since 2016's Tropical Storm Agatha was named on 2 July. The final named storm, Raymond, dissipated on 17 November. Four

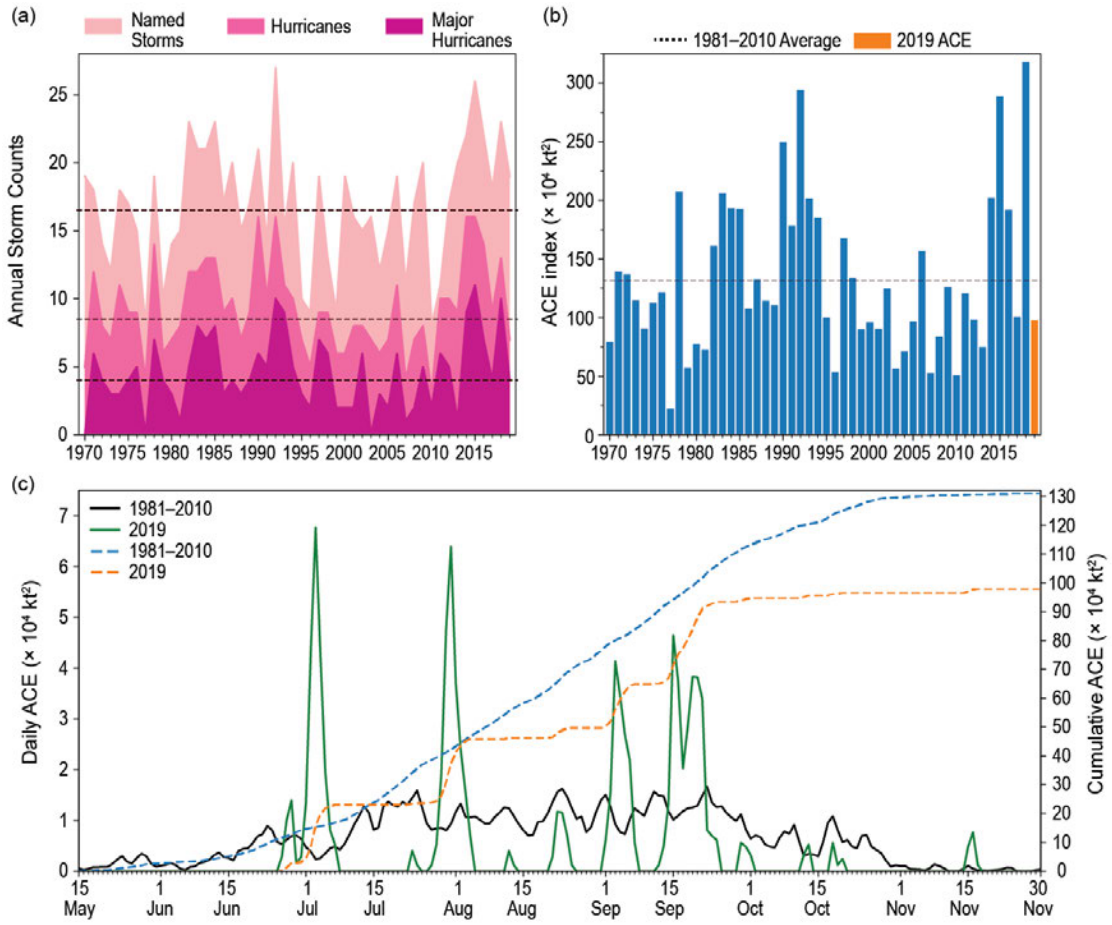

Fig. 4.24. (a) Annual storm counts for the eastern North Pacific by category during 1970–2019, with 1981–2010 average denoted as dashed lines. (b) Annual ACE during 1970–2019, with 2019 in orange and the 1981–2010 average denoted by the dashed line. (c) Daily ACE during 1981–2010 (solid black) and 2019 (solid green); accumulated daily ACE during 1981–2010 (dashed blue) and 2019 (dashed orange).